The tumor-infiltrating B cell response in medullary breast cancer is oligoclonal and directed against the autoantigen actin exposed on the surface of apoptotic cancer cells

Margit H. Hansen*, Heidi Nielsen*, and Henrik J. Ditzel†

Department of Immunology, The Scripps Research Institute, La Jolla, CA 92037

Communicated by Frank J. Dixon, The Scripps Research Institute, La Jolla, CA, August 30, 2001 (received for review June 15, 2001)

Medullary carcinoma of the breast (MCB) is a morphologically and biologically distinct subtype of human breast cancer that, despite cytologically anaplastic features, has a more favorable prognosis than other types of breast cancer at similar stages of differentiation. It has been proposed that the improved clinical outcome is due, at least in part, to the presence of a prominent lymphoplasmacytic cell infiltrate in the tumor stroma. We studied the B lymphoplasmacytic cell infiltrates in MCB to determine the role of the antibody response produced by the local infiltrating cells. Oligoclonal predominance among tumor-infiltrating B cells in a panel of MCB patients was observed, suggesting that certain B cell clones were expanded, possibly in response to specific tumor-associated stimuli. IgG antibody phage-display libraries were generated from MCB-infiltrating lymphoplasmacytic cells of two patients, and MCB-reactive monoclonal antibodies were retrieved by selection on fresh-frozen MCB tissue sections. Analysis by mass spectrometry revealed that the antigen targeted by the dominant clones in the oligoclonal B lymphoplasmacytic response in both patients was not a cancer-specific antigen but the cytoskeletal protein β-actin. MCB exhibits an increased rate of apoptosis, and apoptotic MCB cells were shown to expose actin on the cell surface, permitting its recognition by the humoral immune system. Further, actin fragments, similar to those observed after cleavage with the apoptotic protease granzyme B, were observed in MCB tissue. Our results indicate that the major antibody response produced by tumor-infiltrating B lymphoplasmacytic cells are autoimmune in nature and a consequence of the perturbed state of increased MCB apoptosis caused by granzyme B-induced T cell cytotoxicity and/or intrinsic cellular factors of MCB cells.

medullary carcinoma of the breast | oligoclonality | antibody phage display libraries | apoptosis | human monoclonal antibodies

The immune response, upon manipulation, has been shown to be effective in combating cancer, but the role of the spontaneous immune response in controlling tumor growth and spread remains controversial. For most cancers, the immune system seems to have a limited effect, partially because of low immunogenicity and distortion of various effector functions of the infiltrating immune cells. Interestingly, however, some cancers possess prominent lymphoplasmacytic infiltrates associated with a favorable prognosis, suggesting that effective anti-cancer responses may develop spontaneously. Medullary carcinoma of the breast (MCB), a subtype constituting ≈3–7% of all breast cancers, is an example of such a tumor. MCB is characterized by a set of morphologic criteria originally defined by Ridolfi *et al.* (1), including well circumscribed borders, syncytial growth pattern with absence of glandular pattern, and lymphoplasmacytic cell infiltrates in the tumor stroma. Additionally, MCB cells have large pleomorphic nucleoli, increased mitotic rate, sparse necrosis, and no tubular component. Despite the cytologically anaplastic features and high mitotic rate, the prognosis of MCB is surprisingly better than other types of infiltrating ductal carcinomas, with a 10-year survival of about 84%, significantly higher than patients with non-MCB (63%) (1–5). Because the diagnostic criteria of MCB are very complex and its reproducibility has been questioned, several investigators have tried to simplify Ridolfi's initial diagnostic criteria (1). These changes resulted in increased statistical survival in the MCB group compared with the ductal carcinoma group (2, 3, 5). Interestingly, in these simplified criteria, the lymphoplasmacytic cell infiltrates were always included, demonstrating the importance of this morphologic criterium for improved prognosis.

Several hypotheses have been put forward to explain the biological basis for the favorable prognosis of patients with MCB, including enhanced tumor cell apoptosis (6–8), elevated levels of metastasis-inhibiting factors (6), elevated levels of the adhesion molecule ICAM-1 (9), and the prominence of an effective host immune response (9, 10). The positive correlation between the intensity of lymphoid infiltration and patient survival suggests that the immune system may be involved in restraining the spread of this type of breast cancer. The cells in the immune infiltrate predominantly consist of T, B, and plasma cells. The absence of neutrophils indicates that the tumor-infiltrating leukocytes in MCB are specific stimuli and not a nonspecific inflammatory response caused by tumor necrosis or bacterial agents.

Immunophenotyping of the tumor-infiltrating lymphocytes in MCB has shown a T cell predominance with significantly more granzyme B-positive activated cytotoxic T cells than in poorly differentiated ductal carcinoma (10, 11). The granzyme B-positive activated cytotoxic T cells were often found to be located in close proximity to apoptotic MCB cells. Other studies, however, have found no restrictions in the T cell receptor repertoire, which raised questions about whether lymphoid recruitment *in vivo* is based on T cell receptor recognition (12). The T cell CD8/CD4 ratio in MCB is also not significantly different from that of lymphocytes infiltrating other invasive ductal carcinomas or tumors arising from other anatomic sites (13, 14). Abundant plasma cells are also found in the majority of MCBs, suggesting a role for humoral immunity (1, 10, 14). The plasma cells produce predominantly Ig of the IgG class, in contrast to plasma cells associated with normal breast glands, which produce IgA. Previous studies of the surface light chain phenotypes of the MCB B cell population has demonstrated a predominance of κ-positive cells in the MCB infiltrates, with higher than normal κ:λ ratios (10), generally considered one of the immunophenotypic criteria for clonal expansion.

Because the close proximity between lymphocytes and malignant cells in MCB suggests that the *in situ* lymphoid proliferation is influenced by tumor-related stimuli, defining the antigenic target of

MEDICAL SCIENCES

Abbreviations: MCB, medullary carcinoma of the breast; PI, propidium iodine.

*M.H.H. and H.N. contributed equally to this work.

†To whom reprint requests should be addressed. E-mail: hditzel@scripps.edu.

The publication costs of this article were defrayed in part by page charge payment. This article must therefore be hereby marked "*advertisement*" in accordance with 18 U.S.C. §1734 solely to indicate this fact.

the dominant antibody response generated by these tumor-infiltrating cells may yield valuable insight to the molecular events giving rise to this response. To address this, we analyzed the MCB-infiltrating B lymphoplasmacytic cells and the antibodies produced by these cells at the molecular RNA and protein levels. Herein, we demonstrate that the MCB-infiltrating IgG response is oligoclonal, and antibodies against the autoantigen actin represent the dominant specificity. We further show that actin is exposed on the surface of apoptotic MCB cells, demonstrating the perturbed state that may allow this intracellular antigen to be exposed to the local humoral immune system.

Materials and Methods

V(D)J Analysis and Library Construction. Fresh-frozen tissue from eight patients with typical MCB, fulfilling the criteria of Ridolfi *et al.* (1), were obtained. None had metastasis at time of diagnosis, confounding medical conditions or recurrence of their breast cancer or other malignancies 7 years after surgery. Multiple sections from the lymphoplasmacytic-rich areas of MCB tissue blocks were cut, immediately ground in a guanidinium chloride/mercaptoethanol and RNA isolated. The hypervariable IgH V(D)J region was amplified by reverse transcriptase–PCR, using an IgHFR3B primer (5′primer 5′-GGACACGGCT[G/C] TGTATTACTG-3′) that hybridizes to the third framework region of the V segment and a JHB primer (3′primer 5′-GCTGAGGAGACGGTGACC-3′) that hybridizes to the consensus sequence of J segments, and the product was separated by electrophoresis by using 6% agarose gels. The DNA from the oligoclonal V(D)J gel bands of patients RH-12 and N-21 were recovered and directly cloned into the pBAD TOPO TA vector (Invitrogen). RNA isolated from the MCB tissues were also used as starting materials for library construction by using the pComb3 and pComb3H M13 surface display systems, as described (15–17).

Antigen Identification. BrCaMz01 MCB cells (a kind gift from Prof. V. Möbus, Universitätsklinikum Ulm, Germany) were lysed in 1% Nonidet P-40 in 25 mM Tris·HCl, pH 8.0, on ice for 30 min, and cellular debris was pelletted by centrifugation. The lysate was filtered through 0.2-μm filters and loaded onto an S200 gel filtration column (Amersham Pharmacia). Elution was performed with PBS at a flow rate of 0.5 ml/min, and 1-ml fractions were collected. One microgram of protein from each sample was mixed with 2× sample buffer, boiled for 5 min, and resolved under denaturing (2% SDS) and reducing (100 mM DTT) conditions on 10% Tris·HCl Ready-Gels (Bio-Rad). Following separation, proteins in the gel were either silver stained (Bio-Rad) or electroblotted onto PVDF membrane (Immobilon P, Millipore). After blocking, the membranes were incubated with human Fabs or mouse antibody, diluted to 1 μg/ml in blocking solution for 2 h at room temperature. After washing, bound antibody was detected with horseradish peroxidase-labeled goat anti-human IgG $F(ab')_2$ antibody (Pierce) or horseradish peroxidase-labeled goat anti-mouse IgG antibody (Pierce) and visualized by using chemiluminescent substrate (SuperSignal, WestPico, Pierce). Protein to be identified by matrix-assisted laser desorption ionization-MS was excised from a silver-stained SDS-gel and subjected to an in-gel trypsin digest (www.masspec.scripps.edu).

Immunocytochemical Analysis Using Confocal Laser-Scanning Microscopy. The MCB cell line MDA-MB-157 and the ductal breast cancer cell line MCF-7 were obtained from the American Type Culture Collection. Cells, cultured on chamber slides, were stained with Fabs, mouse anti-actin antibody (clone C4, Chemicon) or Texas red-phalloidin (Molecular Probes) as described (17). Apoptosis was induced by incubating the cells in suspension with 100 ng/ml tumor necrosis factor α (Upstate Biotechnology) and 1 μg/ml cycloheximide for 3–15 h at 37°C/5% CO_2. Apoptotic cells were detected by the TUNEL method by using either the *in situ* cell death detection kit (Roche) according to manufacturer's instructions, by Annexin V-FITC (PharMingen) staining, or by the APO-BRDU kit (Phoenix Flow Systems, San Diego).

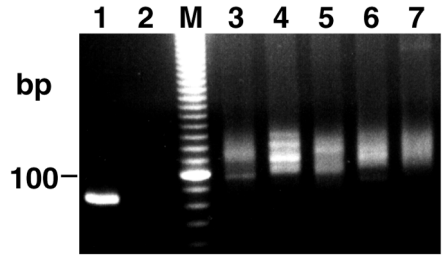

Fig. 1. Analysis of the MCB-infiltrating B lymphoplasmacytic cells demonstrates an oligoclonal response. Amplification of the Ig heavy chain V(D)J segments from four MCB infiltrates (lanes 3, N-1; 4, N-21; 5, RH-12; and 6, RH-2) by reverse transcriptase-PCR and separation by gel electrophoresis resulted in three to five oligoclonal bands in the range of 80–130 bp for each of the tumors. In contrast, V(D)J amplification of a polyclonal B cell population obtained from peripheral blood lymphocytes of a healthy individual (lane 7) gave a smear pattern, whereas the V(D)J product of a human monoclonal antibody resulted in a single distinct band (lane 1). The negative control containing primers, but no DNA, is shown in lane 2. M, marker.

Proteolytic Cleavage of Actin. Purified muscle (0.2 μg) and non-muscle actin (0.2 μg) (both Sigma) were incubated with 0.5 unit of caspase-3 (Bivision, Palo Alto, CA) in cleavage buffer (50 mM Hepes, pH 7.4/2 mM EDTA/1% Nonidet P-40/0.1 M NaCl/10% sucrose/10 mM DTT) for 2 h at 37°C and with 12.5–50 mM granzyme B (Alexis, San Diego) with or without 2 mM iodoacetamide (Sigma) in cleavage buffer for 6 h at 37°C. As controls, actin incubated under the same condition with the exception of omitting protease were included. Western blots of cleaved and uncleaved actin preparations and MCB tissues samples were incubated with rabbit or mouse anti-actin antibodies overnight at 4°C, and bound antibody was visualized as described above.

Results

Reverse Transcriptase–PCR Amplification of Ig V(D)J Segments from the MCB-Infiltrating Lymphoplasmacytic Cells Demonstrates Oligoclonal B Cell Populations. Total cellular RNA was isolated from a 0.5-cm^3 block of lymphocyte-rich fresh-frozen MCB tissues of six patients, ensuring representative material. To evaluate whether some B cell clones dominated the lymphoplasmacytic infiltrate in MCB, the hypervariable V(D)J segments of the rearranged Ig heavy chain genes were amplified by reverse transcriptase-PCR and analyzed. Whereas gel electrophoresis of the PCR-amplified V(D)J product from a monoclonal B cell population resulted in PCR products of a discrete size, the PCR-amplified product from a polyclonal B cell population yielded a smear pattern because of size variations among V(D)J segments of different clones. Applying this technique to the cDNA generated from the six MCB infiltrates demonstrated expansion of selective B cell clones in each MCB. As shown in Fig. 1, three to five distinct bands were observed when the V(D)J-amplified products were separated by agarose gel electrophoresis, indicating an oligoclonal response. For example, the PCR products of the MCB specimens RH-12 showed three discrete DNA bands at 85, 100, and 115 bp (Fig. 1, lane 5), the N-21 specimens showed four bands at ≈102, 110, 121, and 130 bp (Fig. 1, lane 4), and the products from N-1 specimens showed three discrete bands with estimated sizes between 88 and 115 bp (Fig. 1, lane 3).

Oligoclonal Predominance Among the MCB-Infiltrating B Lymphoplasmacytic Cells Confirmed by Sequencing. Next, the dominant V(D)J PCR products of RH-12 and N-21 were recovered from the electrophoresis gels and cloned into the pBAD vector, and a

MCB N-21

Group	# of clones	FR3	CDR3	FR4
102 bp				
A1	3	YYCAN	QTWLQLLYFHH	WGQG
A2	2	-----	-E-----F-Q-	----
B1	3	YYCAR	STVRFSFYGMDV	WGQG
110 bp				
C1	5	YYCAR	AAPTMVQGVIMGFDY	WGQG
C2	5	-----	-HG-------A----	----
D1	2	YYCAR	EGGDRGYNYDNWFDP	WGQG
D2	1	-----	-------TF-------	----
D3	1	-----	-------IS------	----
121 bp				
E1	3	YYCAR	DQVVVAATLSNYGMDV	WGQG
F1	3	YYCAR	DFAVDPDRDTEVIPYWIDP	WGQG
G1	2	YYCAR	GTVTIYGVLIMLPAAGHLDS	WGQG
130 bp				
H1	6	YYCAR	DLGDFLSGYYTEEYYYYYGMDV	WGQG
H2	1	-----	---------T----------	----

MCB RH-12

Group	# of clones	FR3	CDR3	FR4
85 bp				
I1	14	YYCAR	LSWFFDL	WGRG
I2	1	-----	M------	----
J1	1	YYCAR	SRYSGSYVHY	WGQG
J2	1	----G	-V----KID-	----
K1	1	YYCAR	LTGDSFDI	WGQG
K2	1	-----	----G---	----
100 bp				
L1	4	YYCVR	DYGSLGSKDLGY	WGRG
M1	2	YYCAR	DPSGSMPYAFDV	WGQG
N1	2	YYCAR	EGHEGSYYGMDV	WGQG
O1	2	YYCAK	ATYSFSLGALDY	WGQG
P1	2	YYCAR	AESGYDYLFDF	WGRG
P2	1	-----	--S-----VEY	--Q-
Q1	2	YYCAR	ESPGFLMGMDV	WGQG
115 bp				
R1	5	YYCAR	GGRMITFGGSS	WGQG
S1	3	YYCAR	EWPQLEVALDY	WGQG
T1	3	YYCTR	SPNDYGDSLDGNAAFDV	WGQG

Fig. 2. Deduced amino acid sequences of the heavy chain V(D)J region of the clones repeatedly retrieved from the oligoclonal bands of the gel electrophoresis-separated MCB samples RH-12 and N-21, as demonstrated in Fig. 1. cDNA from oligoclonal gel bands were cloned into the pBAD TOPO TA vector, and ≈60 random clones from each sample were sequenced.

number of random clones were sequenced. Comparisons of the DNA and deduced amino acid sequences of individual clones within each gel band revealed further grouping based on heavy chain CDR3 sequences. Sixty-five percent (39 of 60) of random clones sequenced from the N-21 tissue (12–20 clones from each of the four clonal bands) had identical sequences or were somatic variants of at least one other clone. For example, among the 14 clones that contained the 110-bp PCR fragment, two groups were identified based on the similarity of CDR3 region sequences: group C (10 clones) and group D (4 clones). Group C could be subdivided into two subgroups (C1, five cases; C2, five cases), whereas group D could be subdivided into three subgroups. Clones belonging to the same subgroup had identical CDR3 sequences, and subgroups within a group only differed by a few amino acids; subgroups C1 and C2 differed by only three amino acids in the CDR3 sequences, and subgroups D1, D2, and D3 differed by only two amino acids. Similarly, 73% (42 of 60) of the clones sequenced from the RH-12 tissue (20 from each of the three clonal bands) had identical sequences or were related somatic variants (Fig. 2). For example, among the 19 clones containing the 88-bp inserts, three groups were identified based on the similarity of CDR3 region sequences; group I consisted of 15 clones, and groups J and K consisted of 2 clones each (Fig. 2). All of the groups were subdivided into two subgroups, as they were somatic variants of one another. Sequence analysis of those clones for which we obtained multiple copies showed that they contained nucleotide differences not resulting in amino acid substitutions or reverse cloning orientation. This indicates that the predominance of these clones was the result of multiple independent cloning events and not caused by cloning artifacts or a result of preferential PCR amplification.

Selection of Antibodies from Phage Display Libraries Generated from the Tumor-Infiltrating Lymphoplasmacytic Cells of Patients with MCB. To determine whether the antibodies produced by the oligoclonal tumor-infiltrating lymphoplasmacytic response were directed against tumor-related antigens, antibody libraries expressed on the surface of filamentous phage were constructed. As starting material for the antibody phage display libraries, total RNA isolated from the tumor-infiltrating lymphocyte-containing MCB biopsies of patients N-21 and RH-12 was used. Because the IgG subclass distribution of the MCB-infiltrating antibody response had demonstrated a predominance of IgG2 in N-21 and IgG1 in RH-12, subclass-specific primers were used for library construction. From RH-12, an IgG1 κ/λ Fab library of $\approx 10^7$ members was constructed in the pComb3 vector, whereas an IgG2 κ/λ Fab library of $\approx 5 \times 10^6$ members in the Comb3H vector was constructed from patient N-21. Because the IgG1 library was cloned into pComb3 and the IgG2 library was cloned into the pComb3H vector, we could ensure that no crosscontamination occurred during selection. The diversity of the two libraries was tested by sequencing the variable heavy and light chain regions of 10 random clones. Some restriction in the diversity of both libraries was observed with one clone identified twice; however, the rest of the clones had completely different sequences. Comparing these sequences from the libraries with those from the V(D)J analysis, we found that one clone from the N-21 library was identical to one of the dominant clones from the V(D)J analysis (group E1). Moreover, a clone from the RH-12 library was identical to one of the dominant clones from the V(D)J analysis (group S1).

We first selected the RH-12 and N-21 phage libraries against fresh-frozen tissue sections of MCB. Following six rounds of selection of the RH-12 library, a significant increase in eluted phage (100-fold) was observed, indicating enrichment of antigen-binding clones. DNA was isolated from selected clones of the last round of panning, and the heavy chain variable genes were sequenced. Seven of 11 clones from the tissue panning with the RH-12 library had the same sequence (named RH63). The V(D)J sequence of the RH63 heavy chain was identical to one of the dominating clones in the V(D)J-amplified 115-bp band. In contrast, the RH63 sequence was not found among the 10 clones that had been sequenced from the unselected RH-12 antibody library, indicating that the amplification of this clone related to its antigen specificity and not to a bias in the library. When the heavy chain sequence of the RH63-like group of clones was analyzed in more detail, many of the clones contained a few nucleotide differences and, in some cases, also amino acid differences, indicating that the clones were somatic variants of one and another (data not shown). Two additional panning experiments on MCB tissue sections by using the RH-12 library were performed. In both cases, the RH63 clone was retrieved, but in addition two other clones, RH49 and RH87, were repeatedly retrieved. The RH49 heavy chain V(D)J sequence was identical to the dominating clone in the V(D)J-amplified 85-bp band (group I1) and the RH87 heavy chain V(D)J sequence was a somatic variant to one of the dominating clones in the V(D)J-amplified 100-bp band (group P2), differing by only one amino acid.

Selection of the N-21 library against MCB tissue section for four rounds also resulted in a significant increase in eluted phage (20-fold). DNA was isolated from selected clones of the last round of panning, and the heavy chain variable genes were sequenced. Three clones, HB21, HB24, and HB28, dominated the sequenced clones. As for the RH63 group of clones, somatic variants were found in the HB21 and HB28 groups. The HB21 heavy chain V(D)J sequence was identical to the dominant clones in the V(D)J-amplified 110-bp band (group D1), the HB24 heavy chain V(D)J sequence was identical to the dominant clones in the V(D)J-amplified 121-bp band (group E1), and the HB28 heavy chain V(D)J sequence was identical to the dominant clones in the V(D)J-amplified 102-bp band (group A1). The heavy chain sequence of the three clones was completely different from the 10 clones that had been sequenced from the unselected N-21 antibody library. The N-21 library was also selected against MCB lysate coated on ELISA wells and against the MCB cell line, MDA-MB-157. Interestingly, the three predominant clones (HB21, HB24, and HB28) were also isolated from the N-21 library by using these selection strategies. In addition, the predominant clone MC6 was retrieved from the latter two selection procedures.

Identification of the Antigen Recognized by the MCB-Infiltrating Antibodies. Soluble Fabs of the three predominant clones from the RH-12 library and the four predominant clones from the N-21 library were expressed in *Escherichia coli* cultures and Fab concentration determined by a capture ELISA. The staining pattern of these Fab fragments was examined by using indirect immunofluorescence analysis and confocal microscopy, showing that all of the Fabs stained monolayers of the permeabilized MCB cell lines, MDA-MB-157 and BrCaMz01, and the ductal carcinoma cell line

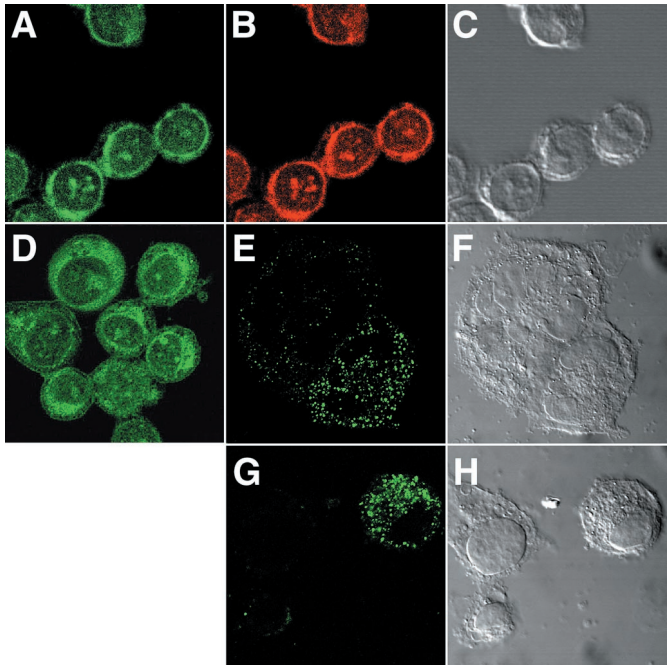

Fig. 3. Staining of ethanol-fixed and permeabilized BrCaMz01 cells (*A–D*) or live BrCaMz01 cells (*E–H*) with Fabs RH63 (*A*, *E*, and *G*) and HB21 (*D*) (green) or Texas red-phalloidin (*B*) (red). Intense cytoplasm staining was observed with both Fabs in the permeabilized cells (*A* and *D*). In contrast, the majority of live non-permeabilized cells were not stained; however, a few cells (*E* and *G*), including some of the cells forming syncytia (*E*), exhibited distinct surface staining and no staining in the cytoplasm. Clear colocalization between the Fabs and phalloidin was observed (*A* and *C*). *C*, *F*, and *H* are differential interference contrast microscopy images of *A*, *E*, and *G*.

MCF7. All seven Fabs exhibited a similar filamentous-type staining pattern of the cytoplasm of all three cell types (Fig. 3 *A* and *D*). In contrast, no staining was seen with control Fabs directed against HIV-1 gp120 (data not shown).

To determine the nature of the cytoplasmic antigen recognized by the selected MCB Fabs, a cytoplasmic BrCaMz01 MCB cell lysate was prepared, and the proteins in the lysate were separated by size exclusion chromatography by using an HR200 column. Next, each protein fraction was tested for binding to selected Fabs (RH63 and HB21) by ELISA and Western blotting (Fig. 4). For Western blotting, 1 μg of protein from each fraction was separated by SDS/PAGE, electroblotted, and subsequently probed with Fabs HB21 and RH63, resulting in staining of a band at a molecular mobility of ≈43 kDa (Fig. 4*A*). To achieve additional separation of the proteins, the two fractions yielding the strongest signals in the Western blots were pooled, concentrated, and again separated by size exclusion chromatography by using an HR75 column. Analysis of the collected fractions by Western blot confirmed one intense band with the mobility of 43 kDa. From a silver-stained gel (Fig. 4*B*), the protein band representing the band appearing on the Western blot of fraction 10 was excised, destained, and examined by using limited proteolysis and matrix-assisted laser desorption/ionization time-of-flight mass spectrometry analysis (Fig. 4*D*). The spectral data were entered into the ProFound protein database to search for the best possible match by using a Bayesian algorithm (18). With the very high Z value of 2.33 (>99.5% probability), the antigen was identified as β-actin, a major component of the microfilament cytoskeleton. The tryptic peptides identified and sequenced were well spread out and covered 34% of the total sequence of β-actin (Fig. 4*E*). The mean error of the measured versus computed masses was less than 20 parts per million. Equally well matched was γ-actin. The two proteins exhibit 96% homology,

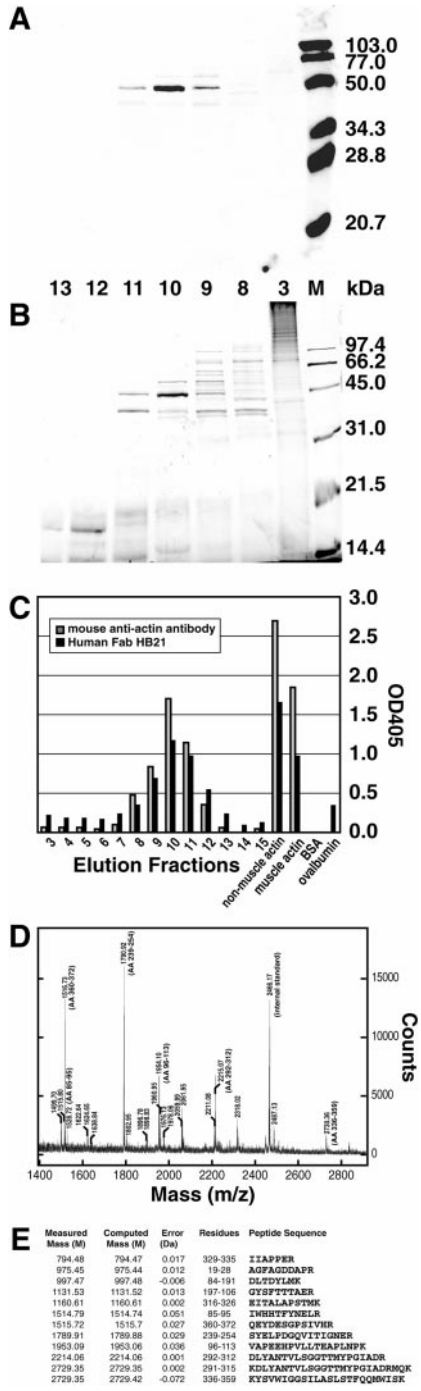

Fig. 4. Identification of the MCB protein recognized by the cloned human anti-MCB antibodies by Western blotting, ELISA, and mass spectrometry. BrCaMz01 MCB cell lysate was separated by size exclusion chromatography and subsequently by SDS/PAGE (fractions 3, 8–13). Gels run in parallel were either (*A*) analyzed by Western blotting (stained with human Fab HB21) or (*B*) silver-stained. M, molecular marker. Western blot analysis revealed binding of Fab HB21 to a ≈43-kDa band in fractions 9–11. The corresponding band from fraction 10 of the silver-stained gel was excised, destained, and analyzed by mass spectrometry identifying β-actin as the MCB protein. No binding to any of the fractions was observed by an anti-HIV-1 gp120 human Fab (negative control). (*C*) The size exclusion fractions (3–15) were also coated on ELISA wells, and the binding of Fab HB21 and a mouse monoclonal anti-actin antibody C4 was measured. In the same ELISA, antibody specificity was examined by binding to purified preparation of nonmuscle actin, muscle actin, BSA, and ovalbumin. (*D*) Mass spectrum from the matrix-assisted laser desorption ionization time-of-flight MS analysis of the peptides derived from the 43-kDa band. The sequences of the β-actin peptides derived from the spectrum are shown in *E*.

and all of the peptides were from the conserved part. To confirm that the band did not contain other proteins, the actin sequences were removed, and the database was searched again with lower stringency. The next protein identified had a Z value of only 0.15, which is not significant, confirming that nonmuscle actin was the only protein present in the band.

To confirm that the anti-MCB antibodies were directed against actin, we tested in parallel a mouse monoclonal anti-actin antibody C4 and the anti-MCB Fabs for their ability to bind to the different size exclusion fractions in ELISA. As shown in Fig. 4*C*, a high correlation between the OD values obtained in the different fractions with the mouse and human antibodies were obtained. In a similar ELISA, sera of 20 healthy individuals were tested for circulating antibodies to actin. None of the healthy donors had anti-actin antibodies in agreement with the findings of others. We also examined colocalization between the cloned anti-actin Fabs and the mouse anti-actin antibody or phalloidin on BrCaMz01 MCB cells. As shown in Fig. 3, complete colocalization between the three anti-actin reagents was observed, with filamentous staining in the cytoplasm and some staining in the nucleus corresponding to the nucleoli.

Actin Is Located on the Cell Surface of Apoptotic MCB Cells. The question remained as to how actin, an intracellular protein, could become exposed to the immune system. Initial experiments examining the staining of Fabs RH63 and HB21 on live BrCaMz01 MCB cells grown on chamber slides revealed that about 3% of the cells exhibited distinct surface staining and no cytoplasmic staining, whereas the remaining cells were not stained (Fig. 3 *E* and *G*). One possible explanation could be that actin becomes exposed on the cell surface during the morphological and biochemical changes that occur when the MCB cells undergo apoptosis. This would allow the immune system to recognize the antigen and perhaps elicit a local immune response within the tumor. Previously, studies have demonstrated an increased frequency of apoptotic cancer cells in MCB (6–8), and in other studies, cytoskeletal alterations including those of cytokeratin, vimentin, and actin have been observed in apoptotic human cancer cells (19, 20). To study whether actin becomes exposed on the surface of apoptotic MCB cells, apoptosis was induced in BrCaMz01 MCB cell cultures by using tumor necrosis factor α and cyclohexamide and subsequently analyzed by confocal laser-scanning microscopy. As shown in Fig. 5 (rows 1 and 2), some of the FITC+ apoptotic cells exhibited surface staining by the anti-actin as shown by the blue Cy5 stain. These cells were morphologically changed, but their cell surfaces were intact, as indicated by the lack of staining with propidium iodine (PI). The anti-actin surface staining was predominantly localized at areas corresponding to the apoptotic cell-surface blebs. In the same view, necrotic cells, as determined by strong staining by PI, were also observed. These cells exhibited neither cell-surface staining with the anti-actin antibody or annexin V, nor intracellularly staining with the anti-actin antibody. This is in correspondence with findings by others that actin in the advanced stages of apoptosis/necrosis is increasingly disintegrated by proteolytic cleavage (20). The confocal analysis also demonstrated that not all cells were apoptotic or necrotic, as completely unstained cells were seen by differential interference contrast microscopy (data not shown). In contrast to the observations with the anti-actin antibody, apoptotic cells incubated with the isotype-matched control antibodies (anti-talin antibody or anti-FLAG antibody) exhibited no Cy5 staining (Fig. 5, row 3).

Actin Fragments, Similar to Those Observed After Cleavage with the Cytotoxic T Cell-Derived Apoptotic Protease Granzyme B, Are Observed in MCB Tissue. We next examined whether actin fragments similar to those observed after cleavage with the apoptotic proteases, granzyme B and caspase-3, were found in MCB tissue.

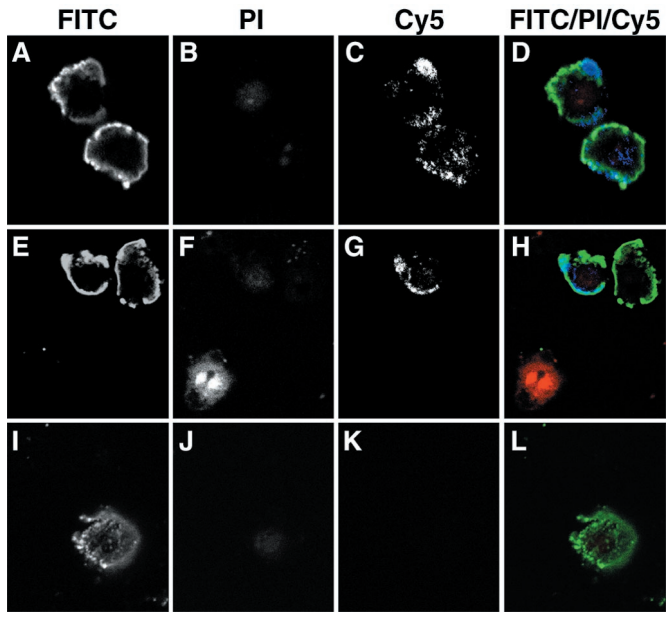

Fig. 5. Actin is exposed on the surface of apoptotic MCB cells, as determined by confocal microscopy. BrCaMz01 MCB cells induced with tumor necrosis factor α and cyclohexamide to undergo apoptosis were incubated with FITC-labeled annexin V (green), PI (red), and an anti-actin antibody or an isotype-matched control antibody (anti-FLAG tag) (blue). The anti-actin antibody (*C* and *G*) and the isotope control (*K*) were detected with Cy5-labeled anti-mouse IgG antibody. PI was included in all of the experiments to ensure the integrity of the membrane throughout the procedure and exclude the possibility that the anti-actin antibodies bound intracellular actin instead of cell surface-exposed molecules. Apoptotic cells were identified by the binding of annexin V to phosphatidyl-serine on the cell surface and the exclusion of the vital dye PI. As seen in *D* and *H*, the anti-actin antibody (blue) stained the cell surface of some of the apoptotic cells (green), whereas necrotic cells (*H*, *Lower*) only exhibited nuclear staining with PI (red), and healthy cells were not stained at all. In contrast, the isotype-matched control antibody exhibited no surface staining of the apoptotic cells (*L*).

Western blots of lysate obtained from fresh-frozen MCB tumors were stained with an anti-actin antibody (Fig. 6, lanes 1 and 2). In the same experiments, we cleaved purified muscle and nonmuscle actin with granzyme B and caspase-3 for comparison. As previously reported, cleavage of actin with caspase-3 yielded fragments with a mobility of 15 and 30 kDa, in addition to 43 kDa of uncut actin. Granzyme B cleavage of actin, which to our knowledge has not been previously reported, yielded a 25-kDa actin fragment. This fragment was observed both in the presence and absence of iodoacet-

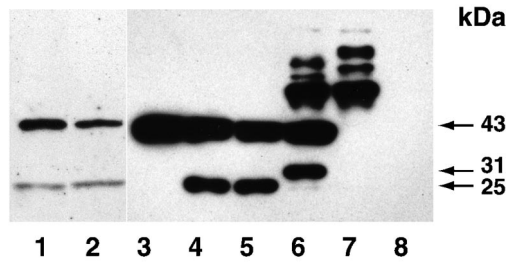

Fig. 6. MCB contain actin fragments similar to those obtained following cleavage with granzyme B. Western blots of tumor lysate obtained from fresh-frozen MCB tumors (lanes 1 and 2) or purified nonmuscle actin either uncut (lane 3), cleaved with 50 mM granzyme B in the presence (lane 4) or absence (lane 5) of iodoacetamide, or caspase-3 (lane 6) were stained for actin. Caspase-3 in the absence of actin (lane 7) yielded some higher molecular weigh background staining, whereas no staining was observed for granzyme B in the absence of actin (lane 8).

amide, which inhibits the activation of caspases by granzyme B. In some experiments, the absence of iodoacetamide resulted in a major 25-kDa band and a minor 30-kDa band, possibly because of caspase-3 activation. A 25-kDa actin cleavage product, similar to that generated by granzyme B in our control experiment, was found in the lysate obtained from fresh-frozen MCB tumors.

Discussion

In this study, we evaluated the nature of the local tumor-infiltrating B lymphoplasmacytic cells in MCB and defined the target of the dominant antibody response produced by these cells. Previous analysis of human systemic immune responses against cancers has led to the identification of a number of tumor-associated antigens (21). The identification of these antigens indicates that at least some cancers are immunogenic. In addition to the so called tumor-associated antibody responses, circulating autoantibodies against several other self-antigens have also been described in cancer patients (22–24). The nature of such autoantibody responses is relatively unknown, partially because most studies have only analyzed crude sera for binding to a panel of cellular antigens, and the antibodies involved in these responses have not been purified or cloned (22, 23). In addition, it is unclear whether these autoantibodies directly relate to the cancer process and/or represent major specificities in the antibody responses. Our study differs significantly from these earlier studies in several aspects: First, we evaluated the clonality and specificity of the local tumor-infiltrating immune response as opposed to the circulating immune response. The close proximity between the infiltrating lymphoplasmacytic cell and the cancer cell clearly demonstrates the relevance of the response. Our analysis showed that the response is oligoclonal, indicating a response generated by specific stimuli. Second, cloning and expression of the dominant antibodies demonstrated the major specificity of the response. Interestingly, the antibody response was directed against the self-antigen β-actin, which is prevalent in most cells, and not a tumor-specific molecule.

Under normal circumstances, actin is not very immunogenic. Previous work has demonstrated that it is very difficult to generate mouse monoclonal anti-actin antibodies because an antibody response is not raised in the mice by normal immunization procedures (25). Most patients with autoimmune disease and antibodies against a variety of antigens do not have antibodies against actin (26). However, some patients with type 1 autoimmune hepatitis have been reported to have anti-actin antibody (26).

Our results suggest that the cause for the anti-actin immune response in MCB relates to the perturbed state within the MCB tumor. Previous studies of MCB tissue demonstrated an increased rate of MCB cell apoptosis (6–8). During apoptosis, a series of morphological changes occurs in which actin has been shown to play an important part (27). Using confocal microscopy and flow cytometry (unpublished observations), we found actin to be exposed on the surface of the apoptotic MCB cells, with staining predominantly corresponding to apoptotic blebs. Interestingly, others have found accumulation of actin at the periphery of apoptotic blebs in permeabilized cells by using phalloidin (20). In these studies, surface staining of actin on nonpermeabilized apoptotic cells was not evaluated. During apoptosis, intracellular proteases are activated, leading to the cleavage of protein substrates. Actin has been found to be a substrate for cleavage of several proapoptotic cysteine proteases both *in vitro* and *in vivo* (28, 29). One of the apoptotic proteases, caspase-3 cleaves actin into 15- and 31-kDa fragments (29). Interestingly, caspase-3, may be cleaved and activated by the LAK- and CTL-specific protease, granzyme B (30). However, granzyme B has also been shown to directly cleave a number of different autoantigens (31), although its effect on actin, to our knowledge, has never been evaluated. We found that granzyme B cleaves actin into 25-kDa fragments and that lysate obtained from fresh-frozen MCB tissue, in addition to intact 43-kDa actin, also contained the 25-kDa actin fragment. This suggests that granzyme B, indicative of the CTL-mediated apoptotic process, may play an important role in MCB. Such fragmentation may diminish the ability of G-actin to be polymerized to F-actin and also may abrogate its ability to inhibit DNase I, a process that occurs early in apoptosis and has been implicated in the formation of plasma membrane blebs (27). It seems likely that the surface exposure of actin, either as aggregates or fragmented molecules, in the context of other apoptotic proteins may render actin immunogenic. Similarly, other investigators have identified other intracellular antigens that were also exposed on surface blebs of apoptotic cells and elicited autoantibodies (32).

In summary, our results add to the increasing body of evidence indicating that autoantibodies are elicited at the perturbed state of apoptosis in cancer and autoimmune disease and demonstrate how clonal analysis and antibody phage display technology can be used to dissect a local immune response. Further elucidation of the cellular arm of the immune response in MCB and the biological features intrinsic to these cancer cells, presumably both partially responsible for the increased apoptotic rate, should give clues to the favorable prognosis of MCB.

We thank Dennis Burton, Lloyd Old, Yao-Tseng Chen, and Paul Parren for helpful discussions and Kim Duffy for technical assistance. This work was supported by California Breast Cancer Research Program Grant 4JB-001 and by the Danish Cancer Society.

1. Ridolfi, R. L., Rosen, P. P., Port, A., Kinne, D. & Mike, V. (1977) *Cancer* **40,** 1365–1385.
2. Wargotz, E. S. & Silverberg, S. G. (1988) *Hum. Pathol.* **19,** 1340–1346.
3. Jensen, M. L., Kiaer, H., Andersen, J., Jensen, V. & Melsen, F. (1997) *Histopathology* **30,** 523–532.
4. Rapin, V., Contesso, G., Mouriesse, H. I., Bertin, F., Lacombe, M. J., Piekarski, J. D., Travagli, J. P., Gadenne, C. & Friedman, S. (1988) *Cancer* **61,** 2503–2510.
5. Pedersen, L., Zedeler, K., Holck, S., Schiødt, T. & Mouridsen, H. T. (1991) *Br. J. Cancer* **63,** 591–595.
6. Jensen, V., Jensen, M. L., Kiaer, H., Andersen, J. & Melsen, F. (1997) *Virchows Arch.* **431,** 125–130.
7. Kajiwara, M., Toyoshima, S., Yao, T., Tanaka, M. & Tsuneyoshi, M. (1999) *J. Surg. Oncol.* **70,** 209–216.
8. Yakirevich, E., Maroun, L., Cohen, O., Izhak, O. B., Rennert, G. & Resnick, M. B. (2000) *J. Pathol.* **192,** 166–173.
9. Bacus, S. S., Zelnick, C. R., Chin, D. M., Yarden, Y., Kaminsky, D. B., Bennington, J., Wen, D., Marcus, J. N. & Page, D. L. (1994) *Am. J. Pathol.* **145,** 1337–1348.
10. Gaffey, M. J., Frierson, H. F., Mills, S. E., Boyd, J. C., Zarbo, R. J., Simpson, J. F., Gross, L. K. & Weiss, L. M. (1993) *Mod. Pathol.* **6,** 721–728.
11. Yakirevich, E., Izhak, O. B., Rennert, G., Kovacs, Z. G. & Resnick, M. B. (1999) *Mod. Pathol.* **12,** 1050–1056.
12. Mathoulin, M. P., Xerri, L., Jacquemier, J., Adelaide, J., Parc, P. & Hassoun, J. (1993) *Cancer* **72,** 506–510.
13. Ben-Enza, J. & Sheibani, K. (1987) *Cancer* **59,** 2037–2041.
14. Jacquemier, J., Piana, L., Torrente, M. & Hassoun, J. (1987) *Breast Cancer* **2,** 212–220.
15. Burton, D. R., Barbas, C. F., III, Persson, M. A. A., Koenig, S., Chanock, R. M. & Lerner, R. A. (1991) *Proc. Natl. Acad. Sci. USA* **88,** 10134–10137.
16. Ditzel, H. J., Binley, J. M., Moore, J. P., Sodroski, J., Sullivan, N., Sawyer, L. S. W., Hendry, R. M., Yang, W. P., Barbas, C. F., III, & Burton, D. R. (1995) *J. Immunol.* **154,** 893–906.
17. Ditzel, H. J., Masaki, Y., Nielsen, H., Farnes, L. & Burton, D. B. (2000) *Proc. Natl. Acad. Sci. USA* **97,** 9234–9239.
18. Zhang, W. & Chait, B. T. (2000) *Anal. Chem.* **72,** 2482–2489.
19. Bursch, W., Hochegger, K., Torok, L., Marian, B., Ellinger, A. & Hermann, R. S. (2000) *J. Cell Sci.* **113,** 1189–1198.
20. Spano, A., Sciola, L., Monaco, G. & Barni, S. (2000) *Eur. J. Histochem.* **44,** 255–267.
21. Boon, T. & Old, L. J. (1997) *Curr. Opin. Immunol.* **9,** 681–683.
22. Fernandez-Madrid, F., VandeVord, P. J., Yang, X., Karvonen, R. L., Simpson, P. M., Kraut, M. J., Granda, J. L. & Tomkiel, J. E. (1999) *Clin. Cancer Res.* **5,** 1393–1400.
23. Vainio, E., Lenoir, G. M. & Franklin, R. M. (1983) *Clin. Exp. Immunol.* **54,** 387–396.
24. Cote, R. J., Morrissey, D. M., Houghton, A. N., Beattie, E. J., Oettgen, H. F. & Old, L. J. (1983) *Proc. Natl. Acad. Sci. USA* **80,** 2026–2030.
25. Sheth, B., Banks, P., Burton, D. R. & Monk, P. N. (1991) *Biochem. J.* **275,** 809–811.
26. Czaja, A. J., Cassani, F., Cataleta, M., Valentini, P. & Bianchi, F. B. (1996) *Hepatology* **24,** 1068–1073.
27. Kayalar, C., Ord, T., Testa, M. P., Zhong, L. T. & Bredesen, D. E. (1996) *Proc. Natl. Acad. Sci. USA* **93,** 2234–2238.
28. Brown, S. B., Bailey, K. & Savill, J. (1997) *Biochem. J.* **323,** 233–237.
29. Mashima, T., Naito, M., Noguchi, K., Miller, D. K., Nicholson, D. W. & Tsuruo, T. (1997) *Oncogene* **14,** 1007–1012.
30. Darmon, A. J., Nicholson, D. W. & Bleackley, R. C. (1995) *Nature (London)* **377,** 446–448.
31. Casiola-Rosen, L., Andrade, F., Ulanet, D., Wong, W. F. & Rosen, A. (1999) *J. Exp. Med.* **190,** 815–826.
32. Casciola-Rosen, L. A., Anhalt, G. & Rosen, A. (1994) *J. Exp. Med.* **179,** 1317–1330.